Par4 is required for platelet thrombus propagation but not fibrin generation in a mouse model of thrombosis

Erik R. Vandendries*†, Justin R. Hamilton‡§, Shaun R. Coughlin‡¶, Bruce Furie*, and Barbara C. Furie*‖

*Division of Hemostasis and Thrombosis, Beth Israel Deaconess Medical Center, Harvard Medical School, Boston, MA 02215; and ‡Cardiovascular Research Institute, University of California, San Francisco, CA 94143

Contributed by Shaun R. Coughlin, November 16, 2006 (sent for review September 22, 2006)

Thrombin, a central mediator of hemostasis and thrombosis, converts fibrinogen to fibrin and is a potent platelet activator. Activated platelets provide a surface for assembly of the tenase and prothrombinase complexes required for thrombin generation. The role of thrombin-induced platelet activation in platelet accumulation and its interplay with fibrin deposition during thrombus assembly has not been fully defined. We studied these processes during laser-induced thrombus formation by using real-time digital fluorescence microscopy in mice lacking protease-activated receptor-4 (Par4), which is necessary for thrombin responsiveness in mouse platelets. Juxtamural platelet accumulation immediately after laser injury was not different in wild-type and *Par4*$^{-/-}$ mice. However, subsequent growth of platelet thrombi was markedly diminished in *Par4*$^{-/-}$ mice. At the time of maximal thrombus size in wild type, platelet accumulation was more than 10-fold higher in wild type than in *Par4*$^{-/-}$ mice. P-selectin expression, a marker of platelet activation, was reduced and delayed in *Par4*$^{-/-}$ thrombi. In contrast to platelet activation and accumulation, the rate and amount of fibrin deposition, predominantly intramural and juxtamural in this model, were indistinguishable in *Par4*$^{-/-}$ and wild-type mice. These results suggest that platelet activation by thrombin is necessary for normal propagation of a platelet thrombus at a distance from the injured vessel wall and hence for normal thrombus growth. However, platelet activation by thrombin is unnecessary for initial and limited accumulation of platelets at or near the vessel wall, and this limited accumulation of platelets and/or platelet-independent mechanism(s) of thrombin generation are sufficient for normal fibrin deposition in this model.

blood coagulation | intravital microscopy | P-selectin

Thrombin plays a critical role in hemostasis and thrombosis by mediating fibrin formation and by activating platelets and other cells via protease-activated receptors (PARs). In mice, Par4 is necessary for platelet activation by thrombin (1). *Par4*$^{-/-}$ mice have prolonged tail bleeding times and decreased thrombosis in mesenteric arterioles after ferric chloride injury, and they are protected against pulmonary embolism after i.v. thromboplastin injection (2, 3). The expression pattern of Par4 as well as data from bone marrow reconstitution experiments strongly suggest that the protection against thrombosis seen in *Par4*$^{-/-}$ mice is due to loss of thrombin signaling in platelets rather than in other cell types (4). However, thrombin is only one of multiple platelet activators, thrombin triggers both fibrin formation and platelet activation, and thrombin-activated platelets provide a surface that supports additional thrombin generation. Exactly where, when, and how platelet activation by thrombin is important during the assembly of a thrombus has not been fully defined.

A model in which laser-induced injury of a mouse arteriole triggers the development of a localized thrombus (5, 6) has been used in conjunction with high speed real-time intravital digital fluorescence microscopy to examine the kinetics, localization, and relative quantification of different components of the developing thrombus, including platelets, tissue factor, fibrin, and P-selectin (7–9). Here, we use this system to explore directly, in real time, the roles of platelet responses to thrombin during thrombus formation by comparing thrombus formation in wild-type and *Par4*$^{-/-}$ mice. Our results reveal a critical role for thrombin signaling for full platelet activation and for growth of the platelet thrombus away from the vessel wall, but not for formation of the initial juxtamural thrombus or for normal fibrin deposition in this model.

Results

Thrombi in *Par4*$^{-/-}$ mice have reduced platelet accumulation. *Par4*$^{-/-}$ mice are viable and have normal blood counts (2). Platelets isolated from *Par4*$^{-/-}$ mice are unresponsive to thrombin, failing to change shape, secrete ATP, aggregate, or mobilize calcium after incubation with thrombin (2). To determine the role of thrombin-induced platelet activation in thrombus formation *in vivo*, we examined the kinetics of arteriolar thrombus development in real time in the cremaster microcirculation of *Par4*$^{-/-}$ and wild-type mice. Thrombus formation was initiated by laser-induced injury of the arteriolar vessel wall. Platelet accumulation was visualized over 5–6 min after injury by using Fab fragments of anti-CD41 (integrin α_{IIb}) conjugated to the Alexa-488 fluorochrome. Thirty-three thrombi in four wild-type mice and 30 thrombi in three *Par4*$^{-/-}$ mice were generated. In wild-type mice, platelets adhered and accumulated at the site of injury. The thrombus increased in size rapidly between 15 and 90 s after injury, and then decreased in size and stabilized at 3–4 min after injury, as previously observed (Figs. 1 and 2*A*) (7, 9). In *Par4*$^{-/-}$ mice, platelets also adhered to and initially accumulated at the site of injury. However, *Par4*$^{-/-}$ thrombi typically increased in size for only the first 15–20 s after injury, and then they decreased in size or stabilized and did not undergo the rapid growth phase seen in wild-type thrombi (Figs. 1 and 2*A*).

A comparison of the rate and extent of platelet accumulation in wild-type and *Par4*$^{-/-}$ thrombi (Fig. 2) support the preceding qualitative description. In wild-type mice, the median time to the half-maximal platelet accumulation was 45 s, and the median time to maximal thrombus size was 74 s after injury. In contrast, in *Par4*$^{-/-}$ mice, the median time to half-maximal platelet

Author contributions: E.R.V., J.R.H., S.R.C., B.F., and B.C.F. designed research; E.R.V. and J.R.H. performed research; J.R.H. and S.R.C. contributed new reagents/analytic tools; E.R.V., B.F., and B.C.F. analyzed data; and E.R.V., S.R.C., B.F., and B.C.F. wrote the paper.

The authors declare no conflict of interest.

Abbreviation: Par4, protease-activated receptor 4.

†Present address: Parexel International, 200 West Street, Waltham, MA 02451-1163.

§Present address: Monash University, Australian Centre for Blood Diseases, 6th Floor Burnet Building, 89 Commercial Road, Melbourne VIC 3004, Australia.

¶To whom correspondence may be addressed. E-mail: shaun.coughlin@ucsf.edu.

‖To whom correspondence may be addressed at: Beth Israel Deaconess Medical Center, 840 Memorial Drive, Cambridge, MA 02139. E-mail: bfurie1@bidmc.harvard.edu.

www.pnas.org/cgi/doi/10.1073/pnas.0610188104

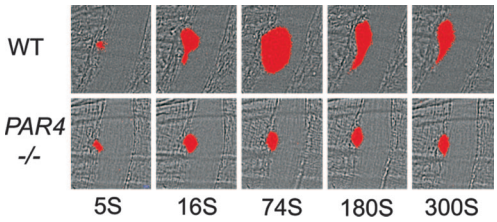

Fig. 1. Thrombosis in cremaster arterioles after laser-induced injury in wild-type and *Par4*$^{-/-}$ mice. Shown are digital fluorescence and brightfield images of representative thrombi in a wild-type (*Upper*) and a *Par4*$^{-/-}$ (*Lower*) mouse at 5, 16, 74, 180, and 300 s after laser-induced injury of the blood vessel wall. Platelets were labeled with anti-mouse CD41 Fab fragments conjugated to Alexa-488. Red pseudo color, platelets.

accumulation was only 5.5 s, and maximal thrombus size was reached by 16 s after injury. At 16 s, again, the time of maximal platelet thrombus size in *Par4*$^{-/-}$ mice but early in thrombus formation in wild type, no statistical difference in the total platelet accumulation was seen between thrombi in wild-type and *Par4*$^{-/-}$ mice (median platelet integrated fluorescence intensity at 16 s was 1.2×10^5 for wild-type mice and 2.5×10^5 for *Par4*$^{-/-}$ mice) (Fig. 2*B*). Thus, *Par4* was not required for initial platelet accumulation. However, wild-type thrombi continued to grow and became significantly larger than *Par4*$^{-/-}$ thrombi (Fig. 2*A*). At the time of maximal platelet accumulation in wild-type mice, median platelet accumulation in wild-type thrombi was 4-fold that in *Par4*$^{-/-}$ thrombi (median platelet integrated fluorescence intensity at 74 s was 1.5×10^6 for wild-type mice and 3.9×10^5 for *Par4*$^{-/-}$ mice; $P < 0.0001$ by the Wilcoxon rank sum test) (Fig. 2*C*).

To further assess the difference in maximal thrombus size between wild-type and *Par4*$^{-/-}$ mice, we examined the quartile distribution of thrombi in both genotypes. All thrombi from both genotypes were placed in rank order of ascending size and the percent of thrombi of each genotype falling into the 1st quartile containing the smallest thrombi, two intermediate quartiles, and the 4th quartile containing the largest thrombi determined. For wild-type mice, 71% of thrombi fell into quartiles 3 and 4, whereas for *Par4*$^{-/-}$ mice, 72% of thrombi fell into quartiles 1 and 2 (Fig. 2*D*). Therefore, although the initiation of platelet accumulation at sites of laser injury appeared normal in *Par4*$^{-/-}$ mice, subsequent platelet accumulation was markedly diminished, resulting in thrombi with significantly reduced size. This finding suggests that Par4-dependent thrombin signaling in platelets is necessary for propagation of the thrombus beyond the juxtamural stage.

P-Selectin Expression Is Delayed and Reduced in Thrombi in *Par4*$^{-/-}$ Mice. To determine the relative importance of thrombin among the other platelet agonists present at sites of thrombus formation *in vivo*, we examined whether the *Par4*$^{-/-}$ platelets that are incorporated into thrombi become activated. As an indicator of platelet activation, we measured extracellular P-selectin exposure, a marker of alpha granule secretion, using Alexa Fluor 488-conjugated anti-mouse P-selectin antibody. Total platelet accumulation was detected with Alexa Fluor 647-conjugated anti-CD41 Fab fragment. After infusion of the labeled antibodies, thrombi were generated by laser injury of the arteriolar wall, and thrombus formation was observed by confocal microscopy to better localize P-selectin fluorescence (Fig. 3*A*). The total integrated fluorescence was quantitated, and the median P-selectin fluorescence, CD41 fluorescence, and P-selectin fluorescence colocalized with and normalized to CD41 fluorescence were determined for 28 thrombi in wild-type mice and 28 thrombi in *Par4*$^{-/-}$ mice. The median ratio of P-selectin fluorescence to CD41 fluorescence was reduced and the appearance of P-selectin delayed in thrombi in *Par4*$^{-/-}$ mice compared with that seen in thrombi in wild-type mice ($P = 0.001$ at 6 min after

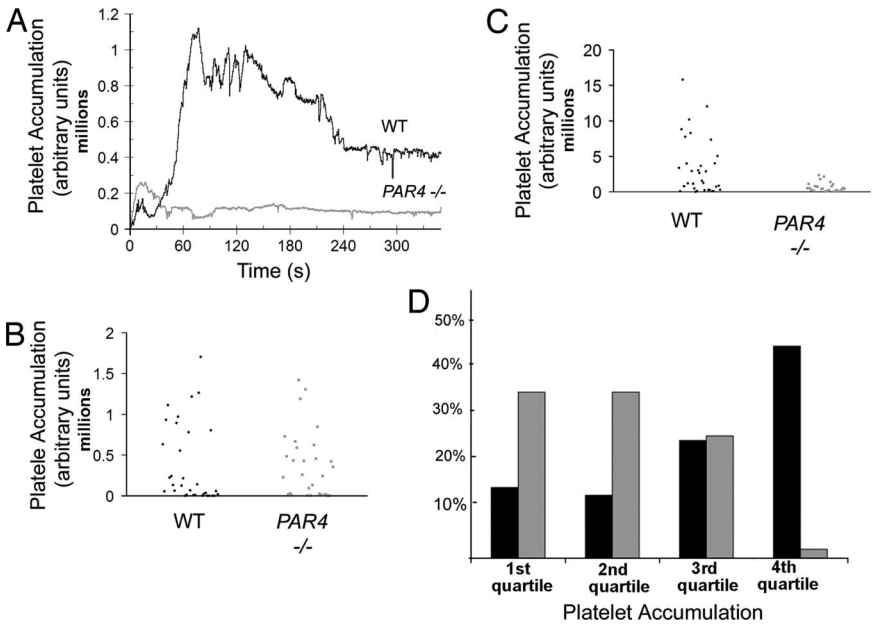

Fig. 2. Platelet accumulation after laser injury in wild-type and *Par4*$^{-/-}$ mice. Platelets were labeled as in Fig. 1. (*A*) Median integrated platelet fluorescence for 33 thrombi in four wild-type mice and for 30 thrombi in three *Par4*$^{-/-}$ mice plotted versus time after laser-induced injury of the cremaster arteriole vessel wall. (*B*) Distribution of the integrated platelet fluorescence for each of the 33 thrombi in wild-type mice and 30 thrombi in *Par4*$^{-/-}$ mice at 16 s after injury. No significant difference is seen between the thrombi in the two genotypes by the Wilcoxon rank sum test ($P < 0.33$). (*C*) Distribution of the integrated platelet fluorescence for each of 33 wild-type and 30 *Par4*$^{-/-}$ thrombi at maximal size. Wild-type thrombi are significantly larger than *Par4*$^{-/-}$ thrombi by the Wilcoxon rank sum test ($P < 0.0001$). (*D*) Distribution of the maximal integrated platelet fluorescence for each thrombus in both genotypes placed in order of ascending thrombus size. Fifty-nine wild-type thrombi and 56 *Par4*$^{-/-}$ thrombi were ranked for determination of the quartile distribution. The percentage of thrombi of each genotype was determined independently in each quartile of the rank order. Black bars, wild-type; gray bars, *Par4*$^{-/-}$.

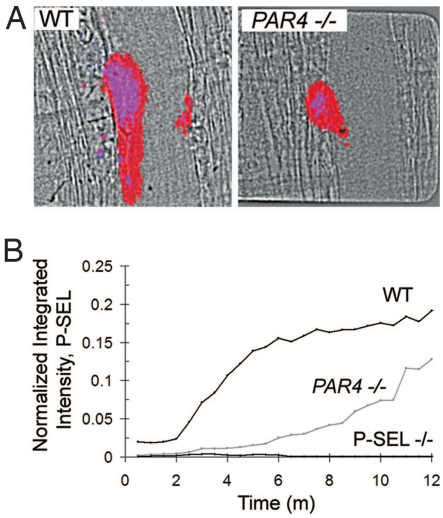

Fig. 3. P-selectin expression in thrombi generated in wild-type and *Par4*$^{-/-}$ mice. Platelets were labeled with Alexa-647-conjugated Fab fragments of anti-mouse CD41 antibodies. P-selectin expression was detected with Alexa-488-conjugated anti-mouse P-selectin antibodies. Confocal fluorescent images (2-μm spacing) were captured every 30 s for 12 min after laser-injury of the arteriolar vessel wall. (*A*) Representative digital fluorescent confocal image of a thrombus in a wild-type mouse and in a *Par4*$^{-/-}$ mouse 6 min after laser injury. Red pseudo color, platelets; blue pseudo color, P-selectin; magenta pseudo color, overlap. For orientation, brightfield images of the corresponding vessels after injury are superimposed on the digital fluorescent images. (*B*) Median platelet specific P-selectin exposure, measured as the integrated anti-P-selectin fluorescence colocalized with anti-CD41 fluorescence divided by the integrated colocalized anti-CD41 fluorescence, plotted as a function of time for each genotype. Twenty-eight thrombi in four mice of each genotype were analyzed for wild-type and *Par4*$^{-/-}$, and seven thrombi in one P-selectin null mouse were analyzed as a control for the specificity of P-selectin antibody. Wild-type and *Par4*$^{-/-}$ thrombi were different at 6 min after injury by the Wilcoxon rank sum test ($P = 0.001$).

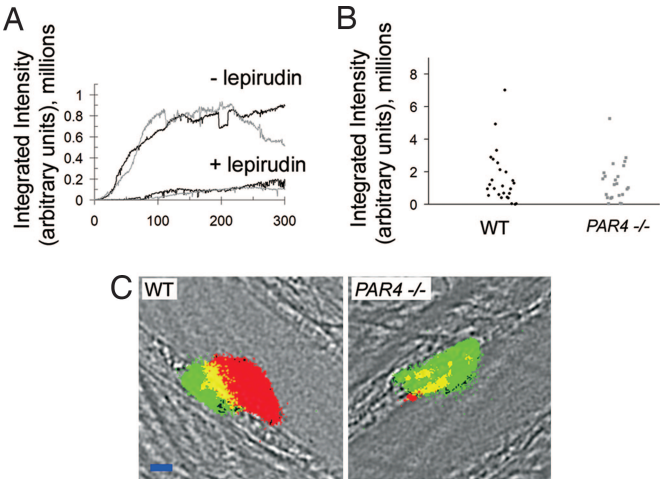

Fig. 4. Fibrin deposition in thrombi in *Par4*$^{-/-}$ and wild-type mice after laser injury. Platelets were labeled as in Fig. 1. Fibrin was detected by using Alexa-647-conjugated anti-human fibrin antibodies. (*A*) For quantification of fibrin deposition, widefield fluorescent images were captured every 500 ms for 5 min after laser injury of the arteriolar vessel wall. The median anti-fibrin antibody fluorescence accumulation of 26 thrombi in four wild-type mice and of 23 thrombi in three *Par4*$^{-/-}$ mice is plotted versus time. The median fibrin accumulation of six thrombi in a wild-type mouse and of five thrombi in a *Par4*$^{-/-}$ mouse determined in the presence of a direct thrombin inhibitor, lepirudin, is also shown. (*B*) Distribution of maximum fibrin deposition of the 26 thrombi in wild-type mice and the 23 thrombi in *Par4*$^{-/-}$ mice. No significant difference is seen between the thrombi in wild-type and *Par4*$^{-/-}$ mice by the Wilcoxon rank sum test ($P = 0.43$). (*C*) Representative digital fluorescent confocal image of a thrombus in a wild-type mouse and a thrombus in a *Par4*$^{-/-}$ mouse 90 s after laser injury. Platelets, fibrin, and overlap are in red, green, and yellow pseudo color, respectively. For orientation, brightfield images of the corresponding vessels after injury are superimposed on the digital fluorescent images.

injury based on the Wilcoxon rank sum test) (Fig. 3*B*). These results suggest that platelets that were incorporated into thrombi in *Par4*$^{-/-}$ mice had defective or delayed activation. Nonetheless, platelet P-selectin was measurable in *Par4*$^{-/-}$ thrombi. Thus, platelet agonists other than thrombin are sufficient to contribute the delayed and diminished platelet activation noted in *Par4*$^{-/-}$ thrombi formed after laser injury.

Fibrin Accumulation Is Normal in the *Par4*$^{-/-}$ Mice. Fibrin accumulation depends on the presence of tissue factor and the subsequent generation of thrombin via the coagulation cascade. It has been hypothesized that activated platelets are important in fibrin generation because of their potential to support assembly of tenase and prothrombinase complexes and to recruit microparticle-borne tissue factor (9, 10). Hence, we wished to determine whether the reduced platelet accumulation and delayed platelet activation seen in *Par4*$^{-/-}$ mice would result in reduced fibrin generation in thrombi generated in these mice. To measure fibrin accumulation, we used an anti-fibrin specific antibody that does not recognize fibrinogen (11). The fibrin antibody was conjugated to Alexa Fluor 647 and was co-infused into mice with the Alexa Fluor 488-conjugated anti-CD41 Fab fragment. Twenty-six thrombi in four wild-type mice and 23 thrombi in three *Par4*$^{-/-}$ mice were generated, and digital widefield fluorescent images were recorded for 5 min after laser-induced injury. While platelet accumulation was significantly reduced in the *Par4*$^{-/-}$ mice, similar to the difference observed in Fig. 1, robust fibrin accumulation was observed. In wild-type mice, fibrin deposition increased during the first 2 min after injury and then stabilized (Fig. 4*A*). The kinetics of fibrin deposition in *Par4*$^{-/-}$ mice was similar to that observed in wild-type mice (Fig. 4*A*). No significant differences were seen between the maximal fibrin generation in thrombi in *Par4*$^{-/-}$ mice compared with the maximal fibrin generation seen in thrombi in wild-type mice (median maximal fibrin integrated fluorescence intensity was 1.0×10^6 in wild-type mice and 1.2×10^6 in *Par4*$^{-/-}$ mice; P value $= 0.43$ by the Wilcoxon rank sum test) (Fig. 4 *A* and *B*). In the presence of lepirudin, a direct thrombin inhibitor, fibrin accumulation was inhibited in both *Par4*$^{-/-}$ and wild-type thrombi (Fig. 4*A*).

To determine the distribution of fibrin and platelets within thrombi, additional thrombi generated in wild-type and *Par4*$^{-/-}$ mice were examined by confocal microscopy. Most of the fibrin deposition in the thrombi of wild-type mice appeared near or at the vessel wall/platelet thrombus interface (Fig. 4*C*). There appeared to be only a partial colocalization between fibrin and the platelet thrombus. In *Par4*$^{-/-}$ mice, there was colocalization between the platelet thrombus and the fibrin. However, the fibrin deposition appeared to extend beyond the site of the stabilized platelet thrombus (Fig. 4*C*).

Discussion

In this report, we compared arteriolar thrombosis in *Par4*$^{-/-}$ and wild-type mice. Platelet accumulation at the site of injury in *Par4*$^{-/-}$ mice was qualitatively and quantitatively indistinguishable from wild-type for several seconds after laser injury, suggesting that Par4 is unnecessary for initial platelet accumulation at the site of injury. However, after the initial 15–20 s, thrombi in *Par4*$^{-/-}$ mice did not increase in size, resulting in platelet thrombi that were much smaller than those in wild-type mice and that remained juxtamural. Hence, Par4 appears to be required for the rapid growth phase of platelet accumulation and

for propagation of the platelet thrombus at a distance from the vessel wall after laser-induced injury. Because platelets isolated from *Par4*$^{-/-}$ mice are specifically unresponsive to thrombin (2) and because transplantation of *Par4*$^{-/-}$ bone marrow confers protection in other mouse models of thrombosis (4), the observed decrease in platelet accumulation and thrombus propagation in *Par4*$^{-/-}$ mice is likely due to absence of thrombin responsiveness in platelets. Thrombin activation of platelets triggers fibrinogen binding to $\alpha_{IIb}\beta_3$ integrin on the platelet surface as well as release of ADP and thromboxane A_2 that further amplify platelet activation. These events promote both formation and stabilization of platelet aggregates. Thus, the decreased platelet thrombus growth in *Par4*$^{-/-}$ mice is likely due to decreased platelet incorporation into the thrombus and/or increased platelet embolization.

Treatment with lepirudin, a thrombin inhibitor, decreased platelet accumulation after laser-injury of the cremaster arterioles to levels seen in *Par4*$^{-/-}$ mice (data not shown). This decrease is in accord with the observation that thrombin inhibition similarly decreased platelet accumulation in a related, but not identical laser-induced model of thrombosis in mesenteric arterioles, at least after severe injuries (12). More importantly, it suggests that prevention of platelet activation by thrombin as opposed to simply prevention of thrombin-mediated fibrin deposition might account for the effects of thrombin inhibition in these models.

The importance of Par4 in thrombus growth has previously been examined in the ferric chloride induced-injury model of arterial thrombosis. Mice deficient in Par4 have decreased occlusion of the mesenteric arterioles secondary to decreased platelet accumulation after injury from ferric chloride (2, 3). Whereas ferric chloride induces the denudation of the endothelium resulting in exposure of subendothelial collagen, the laser-induced injury results in a more localized injury, with undetectable exposure of collagen (5, 13). On the basis of comparisons between ferric chloride-induced thrombosis and laser-induced thrombosis in FcRγ null mice, collagen appears to be important for platelet accumulation after ferric chloride injury but not after laser-induced injury (14). Although the initiating event in thrombus formation in these two thrombosis models is different, thrombin-induced platelet activation plays a role in both, consistent with a general role for thrombin signaling in platelets in propagation of thrombi away from the vessel wall.

The observation that Par4 is required for propagation of the platelet thrombus away from the site of injury but is not necessary for formation of a juxtamural thrombus is interesting in the context of hemostasis in *Par4*$^{-/-}$ mice (2). These mice showed markedly prolonged bleeding times in an assay in which the tail artery and veins were transected and the tail tip was immersed in warm saline (2). Hemostasis in this model demands propagation of a thrombus across the lumen of vessels in the setting of rapid blood flow. Thus, failed hemostasis in this assay is consistent with failed propagation of the platelet thrombus in *Par4*$^{-/-}$ mice. By contrast, *Par4*$^{-/-}$ mice show no evidence of spontaneous bleeding. Thus, day-to-day hemostasis may be achieved by formation of juxtamural thrombi without need for propagation of platelet thrombi across the vessel lumen and/or tamponade provided by surrounding tissue or other mechanisms may mitigate the need for full platelet activation for formation of occlusive thrombi in most settings.

Platelets isolated from *Par4*$^{-/-}$ mice are unresponsive to thrombin but do respond to other platelets agonists (2). In this report we showed that P-selectin exposure on the platelet surface in thrombi in *Par4*$^{-/-}$ mice was delayed and decreased compared with wild-type mice. Thus, thrombin signaling appears to be important for normal activation of even those platelets accumulated in and near the vessel wall. Conversely, some platelets within thrombi in *Par4*$^{-/-}$ mice eventually do become activated. ADP, thromboxane A_2, von Willebrand factor and perhaps collagen below levels of detection by the methods used (6) are candidate agonists for inducing platelet activation in the absence of thrombin signaling. Dubois and colleagues (14) have shown that inhibitors of the ADP receptor and thromboxane reduce the platelet accumulation after laser injury of the cremaster arterioles. In the mesenteric arterioles, by using a related laser-induced injury model, an inhibitor of the P2Y1 receptor was shown to result in a reduction of thrombus size (15). Determining which of these platelet agonists and receptors is responsible for the platelet accumulation and activation seen in the *Par4*$^{-/-}$ mice after laser-induced injury awaits additional studies.

Despite reductions in platelet accumulation and activation at the sites of laser-induced injury in *Par4*$^{-/-}$ mice, no differences in the kinetics or quantity of fibrin accumulation were seen. This finding was surprising because activated platelets have been hypothesized to provide the anionic phospholipid-bearing surface for assembly of the tenase and prothrombinase complexes required for thrombin generation (16). The results reported here suggest that only a subset of the accumulated platelets in a wild-type thrombus may be necessary and sufficient for the level of thrombin generation required to achieve maximal fibrin deposition in this model. In support of this hypothesis, confocal images of wild-type thrombi indicate that fibrin accumulation occurs predominantly along the vessel wall, the site of the limited platelet accumulation in *Par4*$^{-/-}$ mice. It is worth noting that the role of thrombin-activation of platelets in promoting coagulation has been studied primarily *ex vivo* by using human platelets, and the relative importance of this phenomenon may vary by the conditions under which thrombi are formed and by species.

Normal fibrin deposition in *Par4*$^{-/-}$ mice is also consistent with the alternative hypothesis that other membrane surface components of the injured vessel or early thrombus may support thrombin generation, accounting for normal fibrin generation in the face of the decreased accumulation of activated platelets seen in the *Par4*$^{-/-}$ mice. These might include endothelial or other vessel wall cell membranes exposing phosphatidylserine as a consequence of laser-induced injury or circulating cell microparticles bearing exposed phosphatidylserine that are recruited to the injury site. Circulating microparticles have been implicated in thrombosis in a variety of model systems, including in the laser-induced model of thrombosis. We have observed both leukocyte-derived and platelet-derived microparticles accumulating at sites of thrombus formation after laser-induced injury (9) (B.F. and B.C.F. unpublished work).

Last, these studies are consistent with the notion that inhibition of thrombin signaling in platelets may be a useful strategy for preventing cardiovascular events that involve propagation of a platelet thrombus, events that include the acute coronary syndromes and a subset of strokes. The expected sparing of juxtamural thrombus formation that such an approach affords might be advantageous for minimizing risk of bleeding and/or rendering the ruptured or eroded atherosclerotic plaques that trigger acute thrombotic events non-thrombogenic. Of course, the relative importance of thrombin signaling versus other triggers of platelet activation may vary by site, vessel, nature of the injury, and species, but PAR antagonists can prevent the formation of occlusive thrombi in primate carotid injury models of thrombosis (17, 18). These results are consistent with our direct observations of platelet thrombi and the importance of PAR signaling in their propagation and support exploration of PAR inhibition as a possible antithrombotic strategy.

Materials and Methods

Animals. Wild-type C57BL/6J mice and P-selectin null mice (C57BL/6J-Selp^{tm1Bay}) were obtained from The Jackson Laboratory (Bar Harbor, ME). Generation of mice deficient in Par4 (gene designation *F2rl3* or *Par4*) has been described (2). *Par4*$^{-/-}$

mice were backcrossed with C57BL/6J mice for seven generations. The Beth Israel Deaconess Medical Center Institutional Animal Care and Use Committee approved all animal care and experimental procedures.

Antibodies and Reagents. Rat anti-mouse CD41 antibody (clone MWReg30) and rat anti-mouse P-selectin antibody (clone RB 40.34) were from BD Biosciences Pharmingen (San Diego, CA). Mouse anti-human fibrin II β-chain antibody (clone NYBT2G1) was from Accurate Chemical and Scientific (Westbury, NY). Fab fragments from the anti-CD41 antibody were generated by using the ImmunoPure Fab preparation kit from Pierce Biotechnology (Rockford, IL) and then conjugated to Alexa-488 or Alexa-647 according to the manufacturer's instructions (Invitrogen, Eugene, OR). Anti-fibrin antibodies were conjugated to Alexa-488 and Alexa-647, respectively. Lepirudin (Berlex, Montville, NJ) was injected via a jugular catheter at a dose of 8 units/g of mouse 5–15 min before laser-induced injury.

Intravital Microscopy. Male mice were anesthetized with an i.p. injection of ketamine (125 mg/kg; Abbott Laboratories, North Chicago, IL), xylazine (12.5 mg/kg; Phoenix Pharmaceuticals, St. Joseph, MO), and atropine (0.25 mg/kg; American Pharmaceutical Partners, Los Angeles, CA). The mouse was kept at 37°C by using a thermal pad. A tracheal tube was inserted, and a jugular catheter was inserted for administration of anesthesia (Nembutal; Abbott Laboratories), antibodies, and drugs. The scrotum was cut, and the cremaster muscle was exteriorized, pinned over the microscopy stage, and bathed in a 37°C bicarbonate buffered saline aerated with 95% N_2, 5% CO_2. High-speed intravital digital videomicroscopy of thrombus formation was performed as previously described except as indicated below (7). Digital images of thrombus formation were obtained by using an Olympus AX microscope (Olympus, Melville, NY) with a 40 $\times$ 0.8 N.A. water-immersion objective for widefield images and a 60 $\times$ 0.9 N.A. water-immersion objective (Olympus) for confocal images. Widefield images were captured every 500 ms. Confocal intravital microscopy was performed by using a modified Sutter Lambda DG-4 high-speed wavelength changer and a Melles Griot (Carlsbad, CA) 43 Series ion laser for excitation. Confocal images were captured every 2 μm in the z-plane for the entire diameter of the arteriole (typically 30–40 μm) and repeated every 30 s. The system was controlled and the images analyzed by using Slidebook (Intelligent Imaging Innovations, Denver, CO).

Laser-Induced Injury. Arteriole injury in the cremaster muscle was induced by using a nitrogen dye laser (Micropoint Systems, Chicago, IL) tuned to 440 nm, focused through the microscope objective, parfocal with the focal plane, and aimed at the vessel wall. The nitrogen dye laser was pulsed three to five times at 55–65% power depending on the thickness of the cremaster preparation and the size of the vessel. There was no difference between the size of arterioles or the number of laser pulses per injury between the wild-type and Par4$^{-/-}$ mice. In a given mouse, multiple thrombi were induced over a 2-h period. Successive thrombi were generated either upstream of the previous thrombus or in different arterioles within the same cremaster preparation. In wild-type mice, the intra-mouse variation in thrombus size is similar to the inter-mouse variation.

Image Analysis. Image analysis was performed with Slidebook. For widefield fluorescent microscopy, the mean background intensity in each image was calculated as the average pixel intensity in a defined region of the blood vessel just upstream of the injury and developing thrombus. Circulating fluorescent antibody is the major contributor to the mean background fluorescence. The area of the thrombus is defined as the total number of pixels with fluorescence greater than the average maximal upstream fluorescence during the course of the image capture. To correct for background fluorescence, the mean upstream fluorescence intensity multiplied by the area of the thrombus was subtracted from the total fluorescence intensity of the thrombus at each time point. For confocal microscopy, the mean and maximal background vessel fluorescence was defined as the average of the mean and maximal voxel fluorescent intensity in 20 neighboring sections of the vessel before injury formation. The volume of the thrombus was defined as the number of voxels in all planes at a given time point with fluorescence greater than the maximal background fluorescence. As was done with widefield microscopy, background fluorescence was subtracted from the sum fluorescence of the thrombus. In addition, to control for differences in light intensity from the confocal light source, the total fluorescence of the thrombus was normalized to the background vessel intensity by dividing the background-subtracted fluorescence intensity of the thrombus by (the mean background fluorescence $-$ 47). Forty-seven is the mean fluorescence at 0 s exposure. The mean background fluorescence $-$ 47 is directly proportional to the intensity of the light source and to the time of exposure.

This work was supported by grants from National Institutes of Health (to E.R.V., S.R.C., B.F., and B.C.F.) and a C. J. Martin Fellowship from the National Health and Medical Research Council of Australia (to J.R.H.).

1. Coughlin SR (2000) *Nature* 407:258–264.
2. Sambrano GR, Weiss EJ, Zheng YW, Huang W, Coughlin SR (2001) *Nature* 413:74–78.
3. Weiss EJ, Hamilton JR, Lease KE, Coughlin SR (2002) *Blood* 100:3240–3244.
4. Hamilton JR, Cornelissen I, Coughlin SR (2004) *J Thromb Haemostasis* 2:1429–1435.
5. Rosen ED, Raymond S, Zollman A, Noria F, Sandoval-Cooper M, Shulman A, Merz JL, Castellino FJ (2001) *Am J Pathol* 158:1613–1622.
6. Dubois C, Panicot-Dubois L, Merrill-Skoloff G, Furie B, Furie BC (2006) *Blood* 107:3902–3906.
7. Falati S, Gross P, Merrill-Skoloff G, Furie BC, Furie B (2002) *Nat Med* 8:1175–1181.
8. Falati S, Gross PL, Merrill-Skoloff G, Sim D, Flaumenhaft R, Celi A, Furie BC, Furie B (2004) *Methods Mol Biol* 272:187–197.
9. Falati S, Liu Q, Gross P, Merrill-Skoloff G, Chou J, Vandendries E, Celi A, Croce K, Furie BC, Furie B (2003) *J Exp Med* 197:1585–1598.
10. Bevers E, Comfurius P, Zwaal R (1983) *Biochim Biophys Acta* 736:57–66.
11. Kudryk B, Rohoza A, Ahadi M, Chin J, Wiebe ME (1984) *Mol Immunol* 21:89–94.
12. Nonne C, Lenain N, Hechler B, Mangin P, Cazenave JP, Gachet C, Lanza F (2005) *Arterioscler Thromb Vasc Biol* 25:1293–1298.
13. Ni H, Denis CV, Subbarao S, Degen JL, Sato TN, Hynes RO, Wagner DD (2000) *J Clin Invest* 106:385–392.
14. Dubois C, Panicot-Dubois L, Furie B, Furie B (2004) *Blood* 104:842.
15. Hechler B, Nonne C, Roh EJ, Cattaneo M, Cazenave JP, Lanza F, Jacobson K, Gachet C (2006) *J Pharmacol Exp Ther* 316:556–563.
16. Heemskerk JW, Bevers EM, Lindhout T (2002) *Thromb Haemostasis* 88:186–193.
17. Cook JJ, Sitko GR, Bednar B, Condra C, Mellott MJ, Feng DM, Nutt RF, Shafer JA, Gould RJ, Connolly TM (1995) *Circulation* 91:2961–2971.
18. Derian CK, Damiano BP, Addo MF, Darrow AL, D'Andrea MR, Nedelman M, Zhang HC, Maryanoff BE, Andrade-Gordon P (2003) *J Pharmacol Exp Ther* 304:855–861.